OBSERVED HEIGHTS OF EUV LINES FORMED IN THE TRANSITION ZONE AND CORONA

GEORGE W. SIMON

Sacramento Peak Observatory, Air Force Cambridge Research Laboratories, Sunspot, N.M. 88349, U.S.A.

and

ROBERT W. NOYES

Smithsonian Astrophysical Observatory, Harvard College Observatory, Cambridge, Mass. 02138, U.S.A.

(Received 26 July, 1971)

Abstract. The heights of formation of a number of extreme ultraviolet lines in active regions have been measured from OSO-IV spectroheliograms. Using the Lyman continuum at 2000 km above the white light limb as a reference, we find heights for HeI, HeII, CIII, NIII, OIV, OVI, NeVIII, MgX, SiXII, FeXV and FeXVI that are in approximate agreement with models based on analysis of EUV emission intensities. The height of CII is anomalously high. The accuracy of measurement is typically about 2000 km. The data suggest that the transition zone is less steep than calculated from EUV emission intensities; however, higher resolution observations are necessary to resolve the discrepancy.

1. Introduction

With the advent of rocket and satellite observations of extreme ultraviolet (EUV) spectral lines during the past several years, there has been a great increase in the amount of theoretical work concerning the chromosphere-corona transition region. In this narrow zone a few thousand kilometers thick, the temperature rises from 10^4 K to over 10^6 K. The observations and theoretical studies have already given us valuable information on the temperature structure of this region of the solar atmosphere, and of the spectral lines formed therein. However, what have been missing up to now were direct observations of the heights of formation of these spectral lines. These are clearly needed in order to test the various theoretical models which predict the run of temperature vs height in this region.

In this study we have used spectroheliograms obtained by the Harvard experiment on the OSO-IV spacecraft to measure the heights of formation of 15 EUV lines relative to the height of the Lyman continuum, which we assume to be formed 2000 km above the white light limb, at a temperature of 10000 K. Our results were deduced from a simple and purely geometrical argument, as follows: First we measured the locations of bright points in active regions on, for example, a Lyman continuum spectroheliogram, and then computed the distances between pairs of these points. On a second spectroheliogram taken, say, in Mg X 625, within a few hours of the first, we measured distances between the same pairs of bright points. The ratios of the distances obtained from the two spectroheliograms then yield directly the size

Solar Physics **22** (1972) 450–458.

of the Mg X Sun relative to the Lyman continuum Sun. The geometry of the experiment is illustrated schematically for three bright points in Figure 1. It is immediately obvious that there are difficulties with such a technique, primarily because of the weakness of our two main assumptions, first, that the bright points have not moved during the time between the two observations, and second, that all the emission features extend vertically up through the solar atmosphere. A third assumption, that emission comes from a localized height region, is probably justified for transition zone lines but not for pure coronal lines. In addition, it should be emphasized that

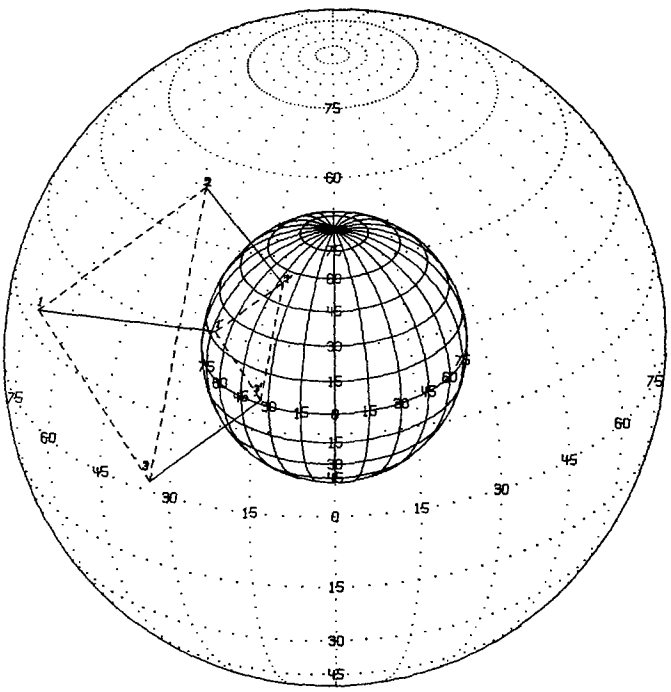

Fig. 1. Two concentric spheres are shown to illustrate the geometry of the experiment. Three points, 1, 2, 3, on the larger sphere, correspond in heliographic position to the points 1′, 2′, 3′, on the smaller sphere. The solid lines 11′, 22′, 33′, are each assumed to lie on a radius of the sphere. The dashed lines 12, 23, 31, 1′2′, 2′3′, 3′1′, are then used to compute distance ratios $R_{12} = 12/1'2'$ etc., which, by the geometry, are equal to the ratios of the radii of the two spheres.

all of our observations refer to active regions only, not to the quiet Sun. It is reasonable to expect the temperature at a given height in active regions to be greater than in neighboring quiet areas, so that the transition zone and coronal lines could be formed somewhat lower in the atmosphere in active regions than in the quiet Sun. (Noyes *et al.*, 1970).

The last and most serious difficulty with the procedure is that the data used have exceedingly low resolution (1 arc min) compared to the precision of location of features on the disk ($\sim$1 arc sec) necessary for good height discrimination. By

averaging and combining the data as described below we are able to increase the precision of position location to the point where meaningful results emerge. With some exceptions these results support the heights of formation deduced from model studies (for example, Withbroe, 1970a; Noyes *et al.*, 1970), which assume hydrostatic equilibrium in the quiet and active Sun.

2. Observations, Analysis, and Results

Full disk spectroheliograms were obtained by the Harvard spectrometer on the OSO-IV satellite between Oct. 27 and Nov. 29, 1967. The instrument and the data are described elsewhere (Reeves and Parkinson, 1967). Usually the instrument obtained spectroheliograms in only one spectral line during each 96 minute orbit of OSO-IV. The scanning time per spectroheliogram was 5.12 min, so that typically some eight to twelve spectroheliograms were recorded during daylight in each orbit. The spacecraft was then commanded to shift to a different spectral line, and the same procedure repeated in the next orbit. In this study we compare spectroheliograms separated in time by one, two, and three orbits; i.e., on the average by about 1.6, 3.2, or 4.8 hrs. Comparisons could also have been made for larger time intervals, but the assumption that bright points remain fixed in the solar surface gets weaker as the interval increases, so we arbitrarily stopped the analysis with three-orbit time differences.

A total of over 1600 spectroheliograms from 278 orbits of OSO-IV were analyzed in this study. In the first two columns of Table I we list the various spectral lines used, and the number of orbits in which each was seen.

The spectroheliometer was designed to scan the 5 mm image of the Sun boustrophedonically with 48 data points recorded in a line, 40 such lines covering the disk. The entrance aperture was a one arc min square, and moved a distance of 22 arc sec in azimuth during the integration time for each point. The angular blur caused by aberration in the off-axis spherical objective mirror was about 15 arc sec. Thus the theoretical resolution function has a half width of 1 arc min in azimuth and elevation, and a tail extending about 27 arc sec in azimuth and 15 arc sec in elevation. Since the data were acquired in digital form, the data reduction was most amenable to computer analysis, which was performed with the Smithsonian Astrophysical Observatory CDC 6400 as described below.

Each spectroheliogram was searched to locate all the bright points (local intensity maxima). In order to qualify as a maximum, each bright point had to meet a number of criteria. For example, in order to eliminate noise spikes and short lived or unstable emission features, we required that the point appear on at least four spectroheliograms during the orbit, that its heliographic coordinates change less than one grid unit in that time, and that it be not too near the limb ($\sin\theta < 0.92$, or $\mu > 0.4$), since limb brightening or darkening can cause errors in the results, as will be discussed later. The point also had to be the brightest in the 5×5 array on which it was centered. (This requirement also implied that no bright points could be less than five grid

units apart). Once a point satisfied all the criteria, the position of the maximum was computed more precisely, by an iterative scheme, using five point Lagrangian interpolation, to a precision of about one arc sec. (We of course do not wish to imply by such precision in computation that there is a corresponding accuracy of measurement for an individual point; however, the reasonableness of the results reported below suggest that the relatively much larger measurement errors are random and can be greatly reduced upon combining all the data). Typically we counted five to twenty bright points on each spectroheliogram. Their coordinates, defined in spacecraft azimuth and elevation units, next were converted into heliographic latitude and longitude. This involved compensating for a number of spacecraft peculiarities. Precession of the spacecraft roll axis and sensitivity changes in the spacecraft Sun sensors, which controlled the size of the spacecraft raster, produced large variations during the 34 day observation period in such parameters as the angle between solar north and the raster axes, the size of the solar image, and the coordinates of the center of the solar disk. Although these were slowly-varying quantities, the instrument also suffered from a large short-term pointing error during each orbit due to thermal effects as the spacecraft heated up when it emerged into daylight. This drift was quite predictable, reaching a maximum at a time $T_{\max}$, about 30 min after sunrise. Its magnitude was typically 15 to 20 arc sec, some 3 to 4 times larger than the position change due to solar rotation during the same time, so it was clearly not negligible. In order to make comparisons between the locations of bright points in successive orbits meaningful, we compared their positions at $T_{\max}$ in the two orbits. Since the position of each bright point was measured on at least four spectroheliograms per orbit, it was possible to determine its position at $T_{\max}$ by a least-squares fit. The reduced data output from each orbit consisted, then, of one heliographic position for each of the bright points.

We next compared the locations of points from two nearby orbits, and after making corrections for solar rotation during the time interval (using the result of Newton and Nunn (1951)), chose those which had not moved more than one grid unit (about one arc min) between the two orbits. As discussed earlier in Section 1, for the two orbits we then computed the ratio of the distances between the points, which is proportional to the ratio of the solar radii in the two spectral lines, and so yields their relative heights of emission. We had intended in every case to compare the radius of a spectral line j to that of the Lyman continuum, i.e., to calculate for each pair of points the ratio $R(j)=\mathrm{D}(j)/\mathrm{D}(\mathrm{Ly})$, where $\mathrm{D}(j)$ is the distance between the pair of points for line j, and Ly refers to the Lyman continuum. In many instances this was possible, but sometimes there were many successive orbits without a Lyman continuum spectroheliogram, and rather than not use these data, we computed instead the ratio between two other spectral lines j and k: $R(j, k)=\mathrm{D}(j)/\mathrm{D}(k)$. Later, when the ratio information from all orbits was combined, we used these results to obtain $R(j)=R(k)\times R(j, k)$ or $R(k)=R(j)/R(j, k)$.

In computing the ratios, we found it necessary to take center-to-limb effects into account. Withbroe (1970a, b) has shown that limb brightening is very significant for

most of the EUV lines studied, and varies considerably from line to line. The Lyman continuum shows limb brightening at the short wave length end and darkening at the long end (Noyes and Kalkofen, 1970). The apparent position of a bright point will be shifted slightly limbward in a limb-brightened line, and centerward in one which shows limb darkening. This effect will produce errors in the computed distance ratios, since our simple geometrical argument will now be even less valid than before. To eliminate this difficulty, we assume that we can express the limb brightening as

$$I(\mu) = I_0 + I_1/\mu \tag{1}$$

where I_0 and I_1 are constants, and that the apparent change in radius of a point is:

$$\Delta r = \gamma \frac{\mathrm{d}I}{\mathrm{d}r}. \tag{2}$$

If r is a dimensionless radius vector with value $r=1$ at the solar limb as seen in the Lyman continuum, then $\mu=\sqrt{1-r^2}$, and

$$\Delta r = \alpha r(1 - r^2)^{-3/2} \tag{3}$$

where γ and α are constants depending on the line under consideration. In polar coordinates, the distance between two points, where θ is the angle between the radii r_1 and r_2 drawn to the points, is

$$\mathrm{D} = (r_1^2 + r_2^2 - 2r_1 r_2 \cos\theta)^{1/2}. \tag{4}$$

But now the true positions r_1 and r_2 appear as $r_1+\Delta r_1$ and $r_2+\Delta r_2$, so that the apparent distance D′ between the points, assuming

$$\frac{\Delta r_1}{r_1} \ll 1 \quad \text{and} \quad \frac{\Delta r_2}{r_2} \ll 1,$$

becomes, to first order in $\Delta r/r$,

$$\mathrm{D}' \approx \mathrm{D}[1 + \alpha f(r_1, r_2, \theta)] \tag{5}$$

where

$$f(r_1, r_2, \theta) = \frac{1}{\mathrm{D}^2}\left\{\frac{r_1^2}{(1 - r_1^2)^{3/2}} + \frac{r_2^2}{(1 - r_2^2)^{3/2}} - r_1 r_2 \cos\theta\left[\frac{1}{(1 - r_1^2)^{3/2}} + \frac{1}{(1 - r_2^2)^{3/2}}\right]\right\}. \tag{6}$$

For two spectral lines we get

$$R'(j, k) = \frac{\mathrm{D}'_j}{\mathrm{D}'_k} \approx \frac{\mathrm{D}_j}{\mathrm{D}_k}\left\{1 + (\alpha_j - \alpha_k)\bar{f}\right\} = R(j, k) + \beta_{jk}\bar{f} \tag{7}$$

where β_{jk} is a constant and $\bar{f}$ is the average of f_j and f_k for the two lines. As $r_1 \to 0$ and $r_2 \to 0$, $f \to 1$, so that the disk-center value of the ratio $R(j, k)$ is obtained from a least-squares fit of R' vs f, using the fitted value of R' when $f=1$.

TABLE I

Heights of formation of EUV lines

Spectral line	Orbits	Weight	Log T (K)	Height (km)	Error (km)
Lyβ 1026	3	60	4.0	3600	2400
Lyγ 972	2	62	4.0	0	1200
Lyε 938	1	25	4.0	3200	2700
Ly Cont	41		4.0	2000[a]	
HeI 584	5	101	4.5	3000	1600
CII 1335	6	117	4.6	10900	1300
HeII 304	9	65	4.9	−700	6500
CIII 977	3	110	4.9	3100	2000
NIII 991	10	283	5.0	3500	2100
OIV 791	16	393	5.2	5100	1000
OVI 1032	19	418	5.5	5100	1900
NeVIII 770	19	555	5.9	8800	1400
MgX 625	84	553	6.2	10600	1600
SiXII 499	32	472	6.4	9400	1700
FeXV 417	10	100	6.5	12800	2200
FeXVI 361	18	138	6.6	15200	2300

[a] By assumption.

Our results are listed in Table I. The weights shown in column 3 are equal to the number of distance ratios measured for each of the spectral lines. All ratios were computed relative to the Lyman continuum, which we assumed to be formed at a temperature of 10000 K at a height of 2000 km above the photosphere. The temperature scale in column 4 is that for maximum abundance of the ion in question, from Allen and Dupree (1969) and Wood and Dupree (1968). The errors are standard deviations in the mean, and are typically on the order of 2000 km. These results are shown graphically in Figure 2, a plot of height vs log temperature. The center of each rectangle in the figure is at the location given in columns 4 and 5 of Table I; the extent along the height axis corresponds to two times the error in column 6. The extent in temperature is the range over which the fractional abundance of the ion exceeds half its maximum value (Allen and Dupree, 1969; Wood and Dupree, 1968) for doubly ionized and higher ions. For the neutral and singly ionized ions, which are generally optically thick, the temperature range is arbitrarily set at 0.1 in $\log T$.

Also in the figure we have plotted the run of $T(h)$ for $T > 10^5$ K deduced for the quiet and active Sun from observed emission measures (Withbroe, 1970a; Noyes *et al.*, 1970). The height of the steep transition zone at 10^5 K is rather arbitrary in these models; here we have set it at 3200 km, 1200 km above the Lyman continuum limb, to agree with the NIII and CIII points at 10^5 K. The plotted points might be expected to lie near the curve for the active Sun if there were no systematic errors and all assumptions used in both methods of height determinations were valid.

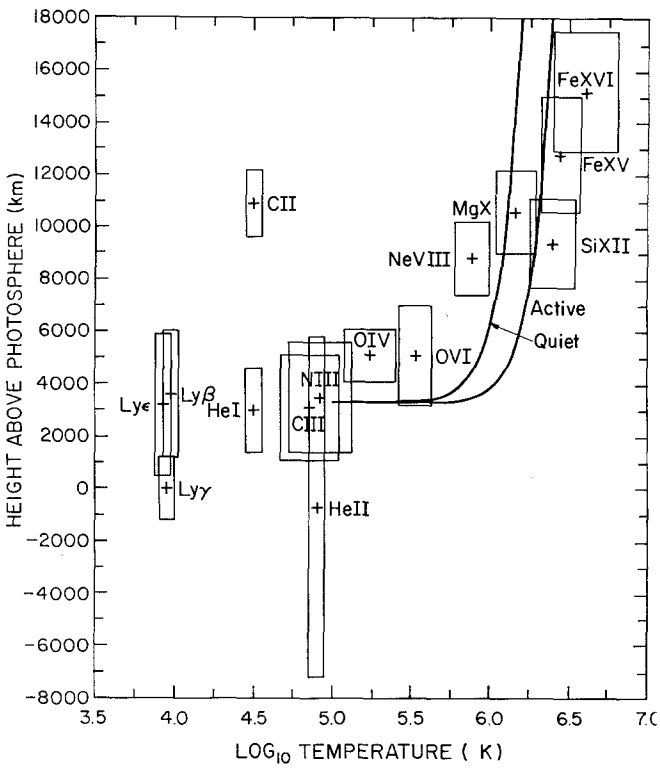

Fig. 2. Measured heights of formation plotted versus temperature of formation, using data from Table I. The temperature range associated with various ions is discussed in the text. Lines labelled ACTIVE and QUIET are models based on EUV intensities, fitted to the present data at $T = 10^5$ K. See text for details.

3. Discussion

The results plotted in Figure 2 clearly reveal the approximate trend of temperature with height in the corona and are in approximate agreement with heights deduced from analysis of EUV intensities. Although the agreement is crude, we find it rather encouraging on two counts:

(a) It demonstrates the ability of this technique to obtain direct height measurements to an accuracy far beyond the instrumental resolution. The uncertainty in height in this work appears to be about 2000 km, some 20 times smaller than the inherent instrumental resolution. This suggests that as new EUV observations become available with higher resolution, the technique may become exceedingly useful.

(b) The results lend support to the assumptions (for example, hydrostatic equilibrium) underlying the analytical technique used to determine models from EUV intensities.

It is interesting that the steepness of the transition zone is not as pronounced in

our results as in the models based on EUV intensities. One possible reason for this difference could be large inhomogeneities in the upper transition zone, such that ions formed above 5×10^5 K (e.g. Ne VIII) are distributed over a range of several thousand kilometers in the low corona. Another possibility of course is some unrecognized systematic error peculiar to Ne VIII which causes it to appear higher than it should.

Such a systematic error clearly has occurred in the determination of the height of formation of C II, which has small error limits but lies higher than other chromospheric lines by several times these limits. We have so far been unable to identify a plausible source for such a systematic error.

One further point of clarification should be added concerning the accuracy of our results. Although we have pointed out that the instrumental resolution is only one arc min, our measurements indicate that the pointing stability of the spacecraft is much better than this, after we compensate for the thermal drift, as discussed earlier. The main effect of the low telescope resolution is to smooth out small-spatial-scale intensity fluctuations which would be seen as discrete elements with higher resolution. However, the locations of these bright points are little affected by this smoothing. This stability in pointing and high accuracy in our position measurements were determined by comparing by least-squares analysis the location of each bright point on successive raster scans during an orbit. These positions typically changed between zero and ten arc sec, and the analysis indicates that the combined effects of pointing instability and telescope smoothing produce an error in our position determinations of 5 to 10 arc sec, not one arc min as implied by the telescope resolution. If this error is then reduced statistically by making 100 to 500 such measurements (cf. column 3 of Table I), it is clear that our quoted accuracy of 2000 km in the results is not unexpected. We cannot, of course, rule out a priori the presence of systematic errors larger than those quoted, which might vary from line to line. However, with the exception of Ne VIII and C II mentioned above, the relatively smooth appearance of our height vs temperature curve in Figure 2 suggests that such systematic errors are probably not important.

In summary, the technique described in this paper, although so far applied only to low-resolution observations, shows great potential for direct measurement of heights of lines formed in the transition zone and corona. Even with the present low resolution data, it provides useful independent information on the nature of the transition zone in active regions.

Acknowledgements

We wish to thank Drs A. K. Dupree, W. Henze, E. M. Reeves, and G. L. Withbroe for valuable discussions, and one of us (GWS) expresses his appreciation to Professor Leo Goldberg for the opportunity to join the Harvard College Observatory as Visiting Associate during which time this research was carried out.

This work was supported in part by the National Aeronautics and Space Administration under Contracts NASW-184 and NAS 5-9274.

References

Allen, J. and Dupree, A.: 1969, *Astrophys. J.* **155**, 27.
Goldberg, L., Noyes, R., Parkinson, W., Reeves, E., and Withbroe, G.: 1968, *Science* **162**, 95.
Newton, H. and Nunn, M.: 1951, *Monthly Notices Roy. Astron. Soc.* **111**, 413.
Noyes, R., Withbroe, G., and Kirshner, R.: 1970, *Solar Phys.* **11**, 388.
Noyes, R. and Kalkofen, W.: 1970, *Solar Phys.* **15**, 120.
Reeves, E. and Parkinson, W.: 1970, *Astrophys. J. Suppl.* **21**, 1.
Withbroe, G.: 1970a, *Solar Phys.* **11**, 42.
Withbroe, G.: 1970b, *Solar Phys.* **11**, 208.
Wood, A., Jr. and Dupree, A.: 1968, Unpublished calculations.